

CHARACTERIZATION OF FILM AFTER IMMERSION TEST IN INDUSTRIAL WHITE LIQUOR*

Luiza Esteves¹

João Henrique Nery Garcia²

Pedro Lana Gastelois³

Waldemar Augusto de Almeida Macedo⁴

Wagner Reis da Costa Campos⁵

Vanessa Freitas Cunha Lins⁶

Abstract

Corrosion testing was performed in white liquor from a Brazilian Kraft mill. Specimens of duplex stainless steel (DSS) and lean duplex (LDSS) were exposed at 170 °C for 30 days to simulate conditions of the digester. Corrosion rates were determined from weight loss measurements. After this exposure, the corrosion products formed on the steel surface was characterized by using scanning electron microscope (SEM) equipped with EDS, X-Ray Diffraction (XRD), and X-ray photoelectron spectrometer (XPS). EBSD can be used to quantify of basis balance phases in DSS and LDSS. General corrosion rates for UNS S32304 LDSS were higher than the UNS 31803 DSS in industrial white liquor at 170 °C for 30 days. XPS and XRD analyses indicated that the film formed after the immersion test may be consisted by Fe and Cr oxides and sulphides.

Keywords: Duplex stainless steels; Weight loss; Industrial white liquor; Autoclave.

¹ Chemistry Dra., Pos doc, SEIES/CDTN, Comissão Nacional de Energia Nuclear, Belo Horizonte, Minas Gerais, Brazil.

² Chemical Eng., Master student, SEIES/CDTN, Comissão Nacional de Energia Nuclear, Belo Horizonte, Minas Gerais, Brazil.

³ Physicist Dr., Technologist, SENAN/CDTN, Comissão Nacional de Energia Nuclear, Belo Horizonte, Minas Gerais, Brazil.

⁴ Physicist Dr., Researcher, SENAN//CDTN, Comissão Nacional de Energia Nuclear, Belo Horizonte, Minas Gerais, Brazil.

⁵ Mechanical Eng. Dr., Technologist, SEIES/CDTN, Comissão Nacional de Energia Nuclear, Belo Horizonte, Minas Gerais, Brazil.

⁶ Chemical Eng. Dra., Professor, Chemical Engineer Department, Universidade Federal de Minas Gerais, Belo Horizonte, Minas Gerais, Brazil.

1 INTRODUCTION

Duplex stainless steel (DSS) is an attractive class of stainless steel characterized by dual-phase ferrite-austenite microstructure. The microstructure depends on alloy composition and manufacturing process. The elements presented in the alloy can stabilize the ferrite or austenite phase. In order to improve its properties, the phase balance is usually a range between 40% and 60% austenite. DSS combines high strength that comes from the ferrite, with ductility and corrosion resistance from austenite. Hence, DSS is mainly used in the fabrication of offshore oil and gas pipelines, offshore concrete structures, ocean mining machinery, chemical tankers in ships, construction of bridges in cold countries, pulp and paper industries, pipelines, and in desalination plants [1-8].

Chemical pulps are made by cooking (digesting) raw materials, using Kraft process (sulfate) and sulfite processes. The Kraft process is the most dominating chemical pulping process worldwide. In Kraft pulp process, active cooking chemicals (white liquor) are sodium hydroxide (NaOH) and sodium sulfide (Na₂S) [9,10], the operation is at high temperature (about 170 °C) and pressure of 5 to 8.5 bar (72 to 123 psi) is used in delignification during the chip cooking cycle [10-12]. Kraft pulping is economically successful because cooking liquor is recovered and reused in chemical recovery process [13,14]. Moreover, white liquor is considered the most aggressive of the alkaline pulping liquors [4,15].

In pulp and paper industries, equipment originally made of carbon steel or austenitic stainless steel are now being replaced by DSS for technical and economic reasons. However, DSS may become susceptible to general corrosion and stress cracking corrosion in high pH caustic solutions [3,4,15].

The current manuscript aims at evaluating the corrosion behavior of duplex steels in industrial white liquor (WL) simulating a digester in the cooking process. The study was developed by using an autoclave for weight loss during 30 days comparing the standard DSS (UNS S31803) and lean duplex (LDSS) (UNS S32304) in WL provided by a Brazilian paper and pulp mill. The corrosion product on surface after immersion test was studied by using scanning electron microscope (SEM), X-Ray Diffraction (XRD), and X-ray photoelectron spectrometer (XPS). The results of electron back scattered diffraction (EBSD) were compared to other methods to quantify the austenite and ferrite phases on the steels.

2 MATERIAL AND METHODS

The UNS S31803 DSS and UNS S32304 LDSS had the chemical composition given in Table 1 and were received as hot rolled coils with a 3.85 mm thickness sheet, annealed at 1075 ± 25 °C. The length described was maintained parallel to the rolling direction.

Table 1. Chemical composition of the investigated DSS (wt. (%))

Steel	Cr	Ni	Mo	Mn	Si	N	C	Fe
S31803	22.45	5.31	2.63	1.81	0.38	0.11	0.013	Bal.
S32304	22.87	4.20	0.27	1.45	0.20	0.15	0.011	Bal.

2.1 Steel characterization

Electron backscatter diffraction (EBSD) analysis was undertaken to quantify the phases with a scanning electron microscope (SEM, Zeiss Sigma VP) interfaced with a Bruker e-FlashHR detector. The specimens were wet ground with SiC paper up to 2000 grit, and then mechanically polished with diamond paste to 1 μm . Then the final electrochemical polishing performed in a mixed solution of $\text{HNO}_3:\text{H}_2\text{O} = 1:1$ for 20 s at 12 V applied voltage [16]. EBSD analysis post-processing was undertaken with Esprit 2 software.

EBSD analysis, optical microscopy [17] and feriscope FISCHER MP3 [18] were used to quantify the phases on the steels.

2.2 Industrial white liquor

Tests performed in industrial white liquor (WL) provided by Brazilian industry (the liquor was shipped in full container and stored cold to minimize decomposition or oxidation). According to Brazilian standards WL: TTA (total titratable alkali): $140 \pm 10 \text{ g.L}^{-1}$ (as NaOH), EA (effective alkali): $110 \pm 10 \text{ g.L}^{-1}$ (as NaOH), sulfidity: $25 \pm 2\%$, causticizing efficiency: $82 \pm 2\%$, total suspended solids $<100 \text{ mg.L}^{-1}$, and $\text{pH} > 12$.

2.3 Coupon Exposure Tests

The corrosion rate was measured by weight loss method. Samples for the corrosion rate tests had a dimension of 15 mm in length and 10 mm in width. The samples were scraped with SiC paper up to 2000 grit. Then, the samples were cleaned, degreased, dried, and the initial weight, using an analytical balance and its area, measured before mounting. Precautions were taken to avoid any contact between the test samples (Teflon rods) and the autoclave (PTFE jacket) in order to prevent any galvanic effects. Autoclave with a volume of 0.3 L type was constructed using type 316 L stainless steel. Up to 4 samples were tested simultaneously. They were immersed in the autoclave at $170 \pm 5^\circ\text{C}$ for 30 days. There was no agitation. After the experiment, the samples were rinsed with distilled water and acetone, dried, and then reaction products on the metal surface were removed using Clarke's solution which was agitated using an ultrasonic bath for require duration. Final weight was measured and was used to calculate corrosion rate for each sample. It was confirmed that Clarke's solution (with the ratio of 100 mL hydrochloric acid, 20 g antimony trioxide (Sb_2O_3) and 50 g stannous chloride (SnCl_2)) [19,20] neither attacked the base DSS metal during the cleaning time nor affected the final weight measurements [3].

2.4 Characterization

Energy dispersive spectroscopy (EDS) analysis coupled to the scanning electron microscope (FEG-SEM) was performed on a Carl Zeiss Microscopy.

Corrosion products formed on the surface of the steels were characterized by using X-Ray Diffraction (XRD) (Geigerflex Rigaku diffractometer with $\text{CuK}\alpha$ radiation in the conventional Bragg-Brentano (θ - 2θ) symmetric geometry and a 2.5° grazing-angle incidence X-ray diffraction (GIXRD), and collected from 20° to $80^\circ 2\theta$. The

unexposed (standard) UNS 31803 DSS and UNS S32304 LDSS were used to compare to those samples were exposed to industrial WL at 170 °C for 30 days. Spectra interpretation was carried out by comparing standards contained in the database (PDF 02 International Centre for Diffraction Data, ICDD, 2003).

The chemical composition of the films was investigated by X-ray photoelectron spectrometer (XPS) with a monochromatic Al K α radiation source and a hemispherical electron analyzer operation at pass energy of 20 eV. The signal of adventitious C 1s (284.6 eV) was used as a reference for the energy calibration of the survey and the high-resolution spectra. The detailed oxidation states of the elements were obtained from fitting the XPS peaks assuming their shape as a convolution of Lorentzian and Gaussian of different components.

3 RESULTS AND DISCUSSION

3.1 Steel Characterization

Figure 1 shows typical microstructure found in the DSS as received. Austenite (γ) islands are embedded in the ferrite (α) matrix with no other secondary precipitates [1]. The Image pro software by an optical microscope, ferritoscope test, and EBSD analysis were used to determine the contents of austenite and ferrite in DSS and LDSS as received. The results are shown in Table 2. In previous work using the Rietveld refinement [17], the results were similar to ferritoscope test and EBSD analysis. EBSD has been shown to be a useful tool for phase identification on DSS; this technique is based on crystallographic orientation [18].

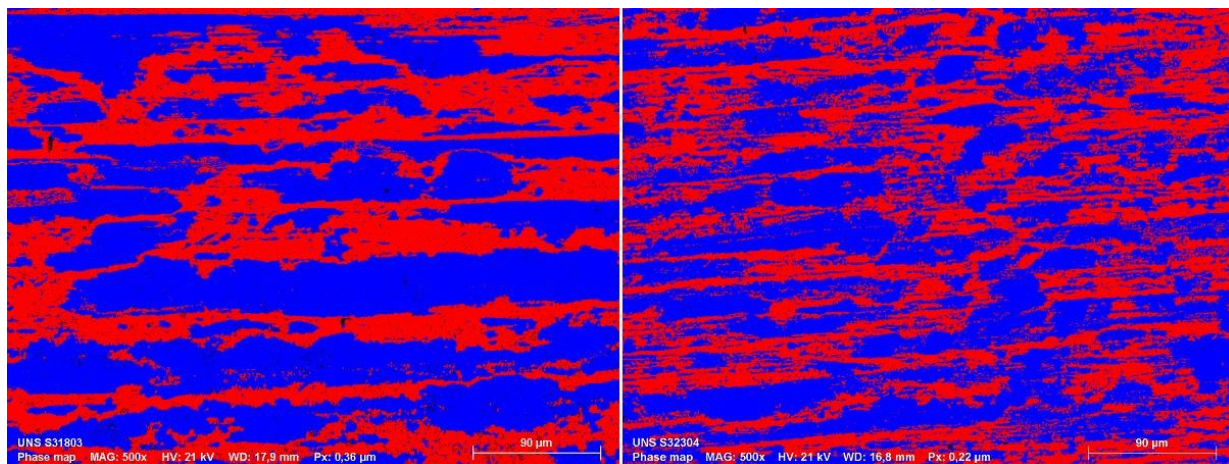


Figure 1. EBSD phases maps: a) UNS S31803 DSS and b) UNS S32304 LDSS, showing ferrite (red) and austenite (blue).

Table 2. Ferrite and austenite content in DSS and LDSS

Steel	Image analysis		Ferritoscope		EBSD analysis	
	Austenite	Ferrite	Austenite	Ferrite	Austenite	Ferrite
S31803	50	50	64	36	56.9	43.1
S32304	46	54	62	38	55.4	44.6

3.2 Weight Loss Measurement

Image analysis by using SEM was performed to confirm the general corrosion, due to uniform distribution of the corrosion products formed on the steels surface, and was not observed selective dissolution of each constituent phase after immersion test for 30 days at 170 °C in industrial white liquor as shown in Figure 2.

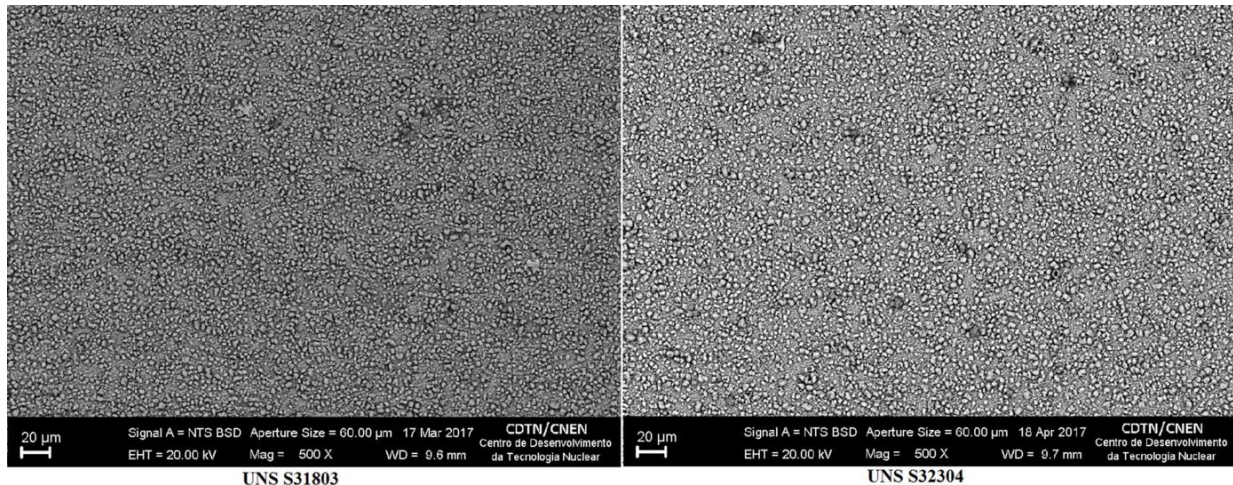


Figure 2. SEM micrograph of (a) UNS S31803 DSS and (b) UNS S32304 LDSS showing the morphology of film formed on the surface of the steels after 30 days immersion test in industrial WL at 170°C.

The corrosion rate can be calculated by the Equation 1, where W is the mass loss (g), A is the area (cm²), t is the time of exposure (s) and d is the density, which was considered 7,9 g cm⁻³ for DSS [21-23].

$$CR = \frac{W}{A \cdot t \cdot d} \quad (1)$$

The average corrosion rates in mm per year (mm/year) for the materials tested were determined from weight loss measurements, and are given in Table 3. General corrosion rates for UNS S31803 DSS were lower than the UNS 32304 LDSS in industrial white liquor at 170 °C for 30 days. This can be attributed to the higher content of alloying elements such as chromium and nickel of the UNS 31803 DSS than in the UNS S32304 LDSS. However, Bhattacharya and Singh (2011) reported UNS 32304 LDSS had the lowest corrosion rate in synthetic white liquor at 170 °C for 15 days [4].

Table 3. Corrosion rates of DSS and LDSS exposed for 30 days in industrial white liquor at 170 °C.

Corrosion rate (mm/year)		
	Average	SD
S31803	0.02	0.01
S32304	0.08	0.02

3.3 Characterization after Weight Loss Experiment

EDS analysis in Figure 3 showed that corrosion products were uniformly distributed on the surface of UNS S31803 DSS and UNS S32304 LDSS. Some precipitates containing elements from the industrial white liquor, such as sodium, calcium, sulfur, and oxygen were observed as shown in Figure 3. Furthermore, iron and sulfur were presented in these precipitates indicating that the corrosion products can be constituted by iron sulfide as related by Bhattacharya and Singh (2011) [4].

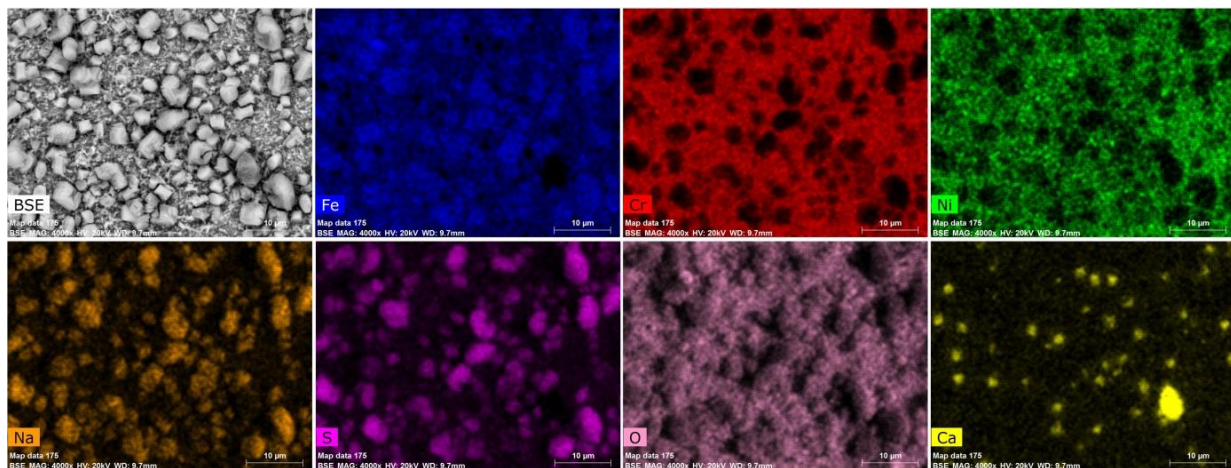


Figure 3. Mapping data obtained by EDS: (a) field of view in S32304, distribution maps of Fe, Cr, Ni, Na, S, O, and Ca.

3.3.1 X-ray diffraction of corrosion products formed on DSS samples in industrial white liquor

Figure 4 and 5 shows the X-ray diffraction pattern with normal (XRD) and 2.5 incidence angle (GIXRD) for DSS and LDSS samples that were unexposed and exposed to industrial white liquor at 170°C for 30 days. According to Bhattacharya and Singh (2011), the XRD at normal incidence the signal depth was about 2-3 µm while the typical passive layer may be a few hundred nanometers. Therefore, the majority of X-ray signals would be from the substrate [4]. Hence, the GIXRD data provides a stronger signal from the film formed on the steel surface than the conventional XRD. The XRD pattern for the unexposed UNS S31803 and UNS S32304 LDSS only showed austenite and ferrite peaks. From the results of GIXRD (Figure 6) for both steels it was quite similar, and the film mainly consisted of magnetite (Fe_3O_4) with some nickel sulphide (NiS_2), which agrees with the study of Bhattacharya and Singh (2011) [4].

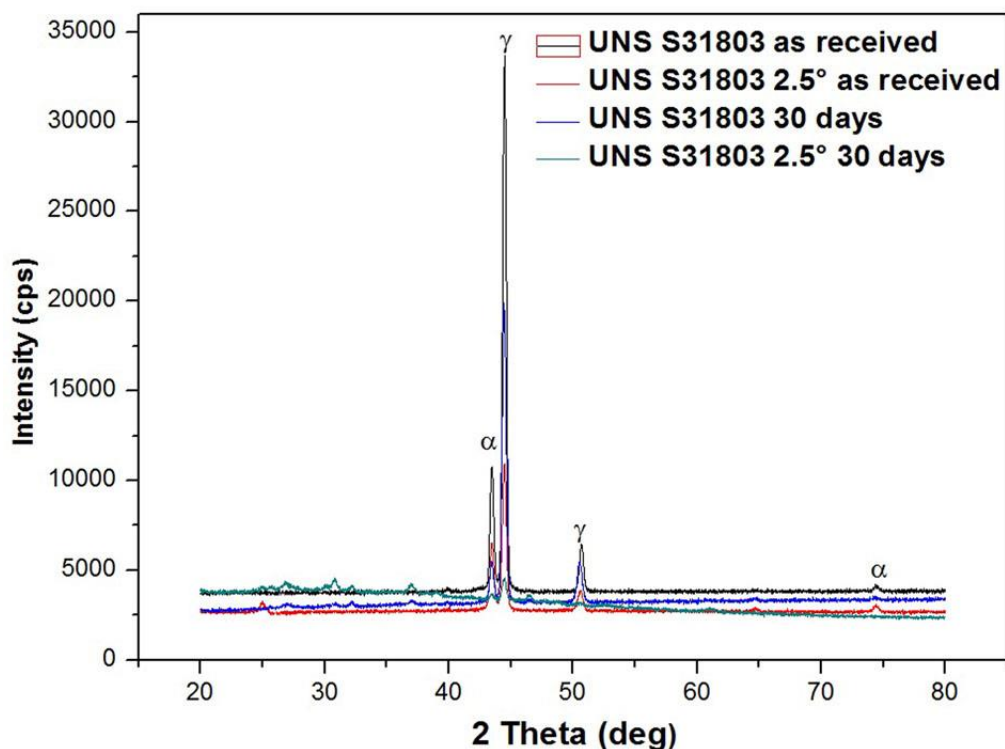


Figure 4. XRD patterns of UNS 31803 DSS base metal and exposed to industrial white liquor at 170 °C for 30 days.

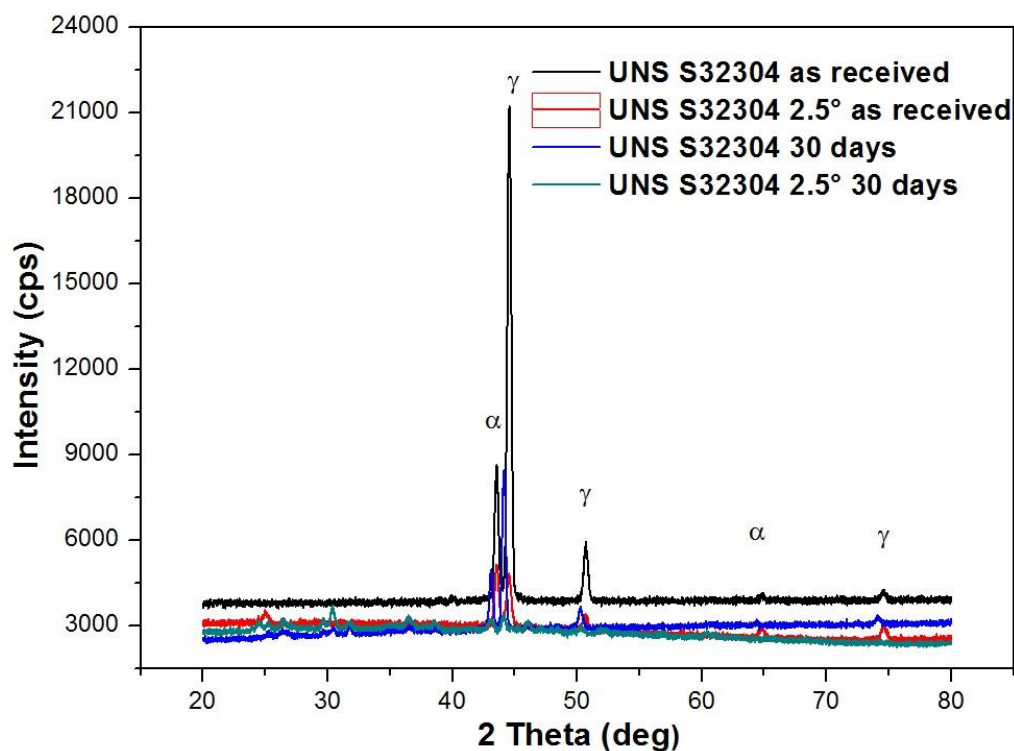


Figure 5. XRD patterns of UNS 32304 LDSS base metal and exposed to industrial white liquor at 170 °C for 30 days.

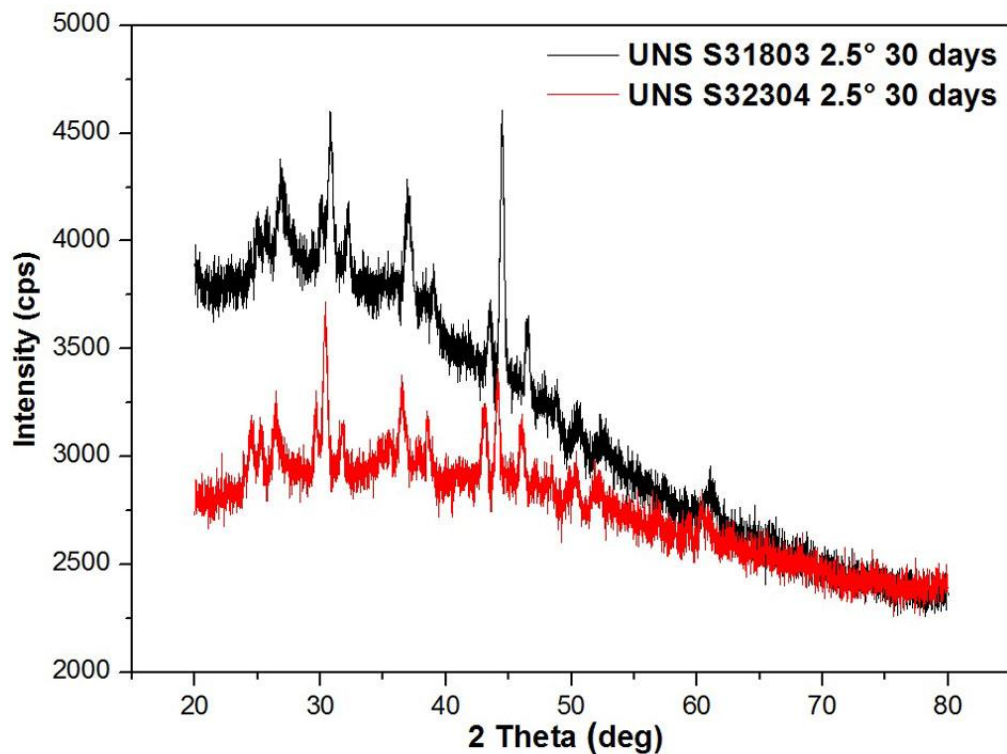


Figure 5. XRD patterns at 2.5° GIXRD of the DSS samples exposed to industrial white liquor at 170 °C for 30 days.

3.3.2 XPS surface analysis

The elemental composition of the oxide surface obtained from the survey scan plotted in Figure 7 reflects, as a whole, the nominal composition of the original duplex stainless steel sample indicating the formation of a larger concentration of Fe and Cr oxides. From the high-resolution spectra, it is noticed large metallic peaks of Fe(0) and Cr(0) before the exposure in industrial white liquor at 170 °C for 30 days, which is an indication of the predominant metallic state that is decreased after immersion test, becoming oxidized species. It could be concluded from XPS analysis that the film formed after the immersion test may present predominantly Fe and Cr oxides and also sulphides.

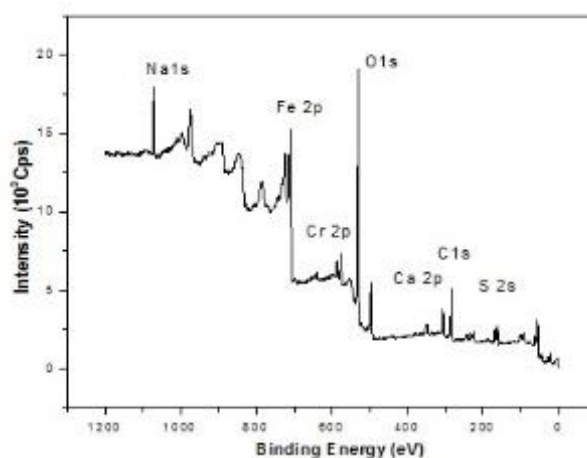


Figure 7. The XPS spectra of the film formed on the UNS S31803 DSS steel surface after 30 days in industrial white liquor at 170 °C.

4 CONCLUSION

- ❖ EBSD was a better tool to quantify the phases on DSS and LDSS.
- ❖ The UNS S31803 DSS had the lowest corrosion rate in industrial white liquor at 170 °C for 30 days.
- ❖ The film was uniformly formed on the steel surface, and it mainly consisted of magnetite (Fe₃O₄) with some nickel sulphide (NiS₂).

Acknowledgments

The authors are grateful to the Brazilian government agencies (CNPq, CAPES, and FAPEMIG) for the financial support for this research and Centro de Desenvolvimento da Tecnologia Nuclear – CDTN for the technical support.

REFERENCES

- 1 Michalska J, Sozańska M. Qualitative and quantitative analysis of σ and χ phases in 2205 duplex stainless steel. Mater Charact [Internet]. 2006 [cited 2015 Jan 5];56(4–5):355–62. Available from: <http://linkinghub.elsevier.com/retrieve/pii/S1044580305002524>
- 2 Westin EM. Microstructure and properties of welds in the lean duplex stainless steel LDX 2101 ® [thesis]. Stockholm: Royal Institute of Technology; 2010.
- 3 Bhattacharya A, Singh PM. Role of microstructure on the corrosion susceptibility of UNS S32101 duplex stainless steel. Corrosion. 2008;64(6):532–40.
- 4 Bhattacharya A, Singh PM. Electrochemical behaviour of duplex stainless steels in caustic environment. Corros Sci [Internet]. 2011. 53(1):71–81. Available from: <http://dx.doi.org/10.1016/j.corsci.2010.09.024>
- 5 Schulz Z, Whitcraft P. Availability and Economics of Using Duplex Stainless Steels. Corros 2014. 2014;(4345):1–10.
- 6 Sahu JK, Krupp U, Ghosh RN, Christ H. Effect of 475 °C embrittlement on the mechanical properties of duplex stainless steel. Material Science and Engineering A. 2009;508:1–14.
- 7 Krauss G. Steel Processing, Structure, and Performance. 1st ed. Vol. 129, ASM International. ASM International; 2005.
- 8 Marcus P, Mansfeld F, Marcus, Philippe Mansfeld F. Analytical Methods In Corrosion Science and Engineering. Taylor & Francis Group; 2006.
- 9 Bajpai P. Biotechnology for Pulp and Paper Processing. Boston, MA: Springer US; 2012 [cited 2015 Jan 8]. Available from: <http://link.springer.com/10.1007/978-1-4614-1409-4>
- 10 Bajpai P. Green Chemistry and Sustainability in Pulp and Paper Industry. Patiala, India. Springer US; 2015.
- 11 Russel EH. Near-infrared spectroscopy for on-line analysis of white and green liquors. Tappi J. 1999;82(9):101–6.
- 12 Hazlewood PE, Singh PM, Hsieh JS. Role of Wood Extractives in Black Liquor Corrosiveness. Corros Eng [Internet]. 2006. 62(10):911–7. Available from: <http://corrosionjournal.org/doi/abs/10.5006/1.3279901>
- 13 Tuthill AH. Stainless Steels and Specialty Alloys for Modern Pulp and Paper Mills. Nickel Dev Inst Ref B Ser. 2002;(11):1–22.
- 14 Wensley A. Pulp and Paper. In: Scully, editor. Corrosion Tests and Standards : Application and Interpretation. 2. ed. West Conshohocken, PA: ASM International; 2005. p. 795–811.
- 15 Wensley A. Corrosion in Alkaline Pulping Liquors. In: NACE. NACE Corrosion 2004 Conference. 2004 May 28-Apr 1; New Orleans, LA. US. Houston: NACE; 2013. p. 1–13.

- 16 Guo LQ, Lin MC, Qiao LJ, Volinsky A a. Ferrite and austenite phase identification in duplex stainless steel using SPM techniques. Appl Surf Sci [Internet]. 2013[cited 2014 Jul 31];287:499–501. Available from: <http://linkinghub.elsevier.com/retrieve/pii/S0169433213016826>
- 17 Esteves L, Lins FC, Viana AK do N, Paiva PRP. Rietveld and Impedance Analysis of Cold and Hot Rolled Duplex and Lean Duplex Steels for Application in Paper and Pulp Industry. Mater Res. 2016;20(1):30–5.
- 18 Michalska J, Chmiela B. Phase analysis in duplex stainless steel: comparison of EBSD and quantitative metallography methods. IOP Conf Ser Mater Sci Eng [Internet]. 2014. 55(1):12010. Available from: <http://iopscience.iop.org/1757-899X/55/1/012010>
- 19 Magnabosco R. Influência da microestrutura no comportamento eletroquímico do aço inoxidável UNS S31803 (SAF 2205) [thesis]. São Paulo: Universidade de São Paulo; 2001.
- 20 Wade, S. Lizama, Y. Clarke's Solution Cleaning Used for Corrosion Product Removal: Effects on Carbon Steel Substrate. In: Australian Corrosion Association. Annual Conference of the ACA: Corrosion & Prevention. Adelaide, South Australia; 2015.
- 21 ASTM, Standard practice for preparing, cleaning, and evaluating corrosion test specimens [standard G1-03], in: ASTM Int. ASTM Handbook 3.02 Corrosion of Metals, Wear and Erosion, West Conshohocken, PA, 2011, 20-28.
- 22 Itman AF, Silva RV, Cardoso W da S, Casteletti LC. Effect of Niobium in the Phase Transformation and Corrosion Resistance of One Austenitic-ferritic Stainless Steel. Mater Res. 2014;17(4):801–6.
- 23 Mattsson E. Basic Corrosion Technology for Scientists and Engineers [Internet]. 2nd Editio. London: The Chameleon Press Ltd; 2001. Available from: <http://books.google.com/books?id=I9JRAAAAMAAJ&pgis=1>
- 24 ASTM. Standard guide for laboratory immersion corrosion testing of metals. ASTM Int. 2012;G31–12a(21200):1–10.